

General Relativistic Precession of the Spin Axis of Binary Pulsar B1913+16: First Two Dimensional Maps of the Emission Beam

Joel M. Weisberg

*Department of Physics and Astronomy, Carleton College, Northfield,
MN, 55057 USA*

Joseph H. Taylor

Department of Physics, Princeton University, Princeton, NJ 08544 USA

Abstract. Relativistic spin-orbit coupling should cause the spin axis of Binary Pulsar B1913+16 to precess at a rate of about 1 deg / yr. As a result, the pulse profile is expected to exhibit secular evolution. Weisberg, Romani, & Taylor (1989), and Weisberg & Taylor (1992) found that the intensity ratio of the two conal components changed at a one percent per year rate from 1981 to 1989, but that their spacing did not measurably change. They attributed these observations to our line of sight passing across the middle of a patchy cone of emission. Recently Kramer (1998) found that the intensity ratio continued its secular change for another decade, and also detected a narrowing of the conal component separation.

We present our analysis of eighteen years of 21 cm pulse profile data. We confirm that the profile is narrowing as precession finally carries our line of sight away from the emission beam axis, and we map the beam in two dimensions. The beam is elongated in the latitude direction, and the degree of elongation grows with radius.

1. Introduction

The spin axis of Binary Pulsar B1913+16 should precess due to metric curvature induced by the companion. This phenomenon, called “geodetic precession,” results from spin-orbit coupling. The calculated rate of precession is 1.21 deg / yr. This precession will cause the observer’s line of sight to slowly drift across the pulsar beam. In the context of the hollow-cone beam model, the separation between the two components that are emitted from opposite sides of the cone should change with time.

Weisberg, Romani, & Taylor (1989), and Weisberg & Taylor (1992) searched for pulse profile changes indicating spin axis precession in data from the 1980’s. They did not detect the expected change in component *separation*, but they found that the relative *strength* of the two components was changing by $\sim 1\%$ / yr. They stated that the constancy of component separation indicated that our line of sight was fortuitously passing near the center of the emission beam, where width changes with latitude are negligible. The component intensity

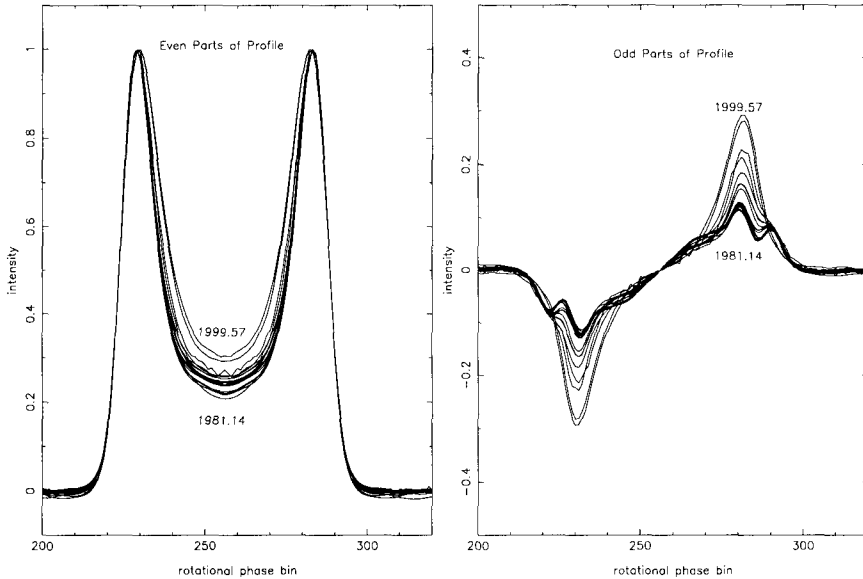


Figure 1. PSR B1913+16 average profiles decomposed into even (left) and odd (right) parts for observing sessions from 1981 to 1999.

changes were ascribed to emission from a patchy cone. Istomin (1991) found that our data suggested that the pulsar will disappear in the year ~ 2020 as the beam precesses away from our line of sight.

Recently, Kramer (1998) observed B1913+16 with the Effelsberg telescope. He combined his data with our older results to find that the component separation had finally begun to change. He modelled the geometry of the system and fit the component separation data to it. Kramer confirmed within the context of his model that the pulsar will disappear in around 2020. (See also Karastergiou et al, this volume.)

We have acquired two years of data since the Arecibo upgrade was completed in 1998 so that we now have eighteen years of high quality data at 21 cm. We use these data for a study of the precession and an analysis of the emission beam. (See Stairs, this volume, for geodetic precession of PSR B1534+12.)

2. Observations and Preliminary Analysis

We have observed PSR B1913+16 at 21 cm generally for two-week sessions approximately annually from Arecibo since 1981. The data were gathered with one of three observing backends, called “Mark I, II, or III,” whose parameters are given in Taylor & Weisberg (1989). The raw data recorded by these systems consist of 5-minute average pulse profiles. We accumulated all such profiles into a “session grand average profile” for each of the observing sessions. Care was taken to make the Mark I, II, and III data as closely intercomparable as possible by simulating some backend hardware operations in software.

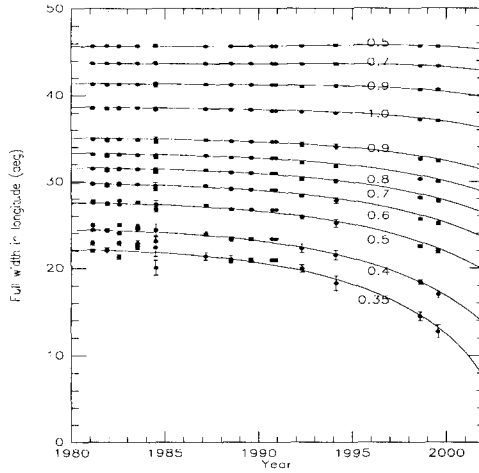


Figure 2. Observed and fitted component spacings at specified constant relative intensities I/I_{max} , as a function of date.

3. Precession and Beamshape Modelling

In order to separate the temporal variations caused by precession and those resulting from the patchy beam, we decomposed each profile into even and odd parts (see Figure 1). We then presumed that the even part represents the overall beam geometry (with assumed east–west symmetry) while the odd part displays the smaller scale beam variations. Our subsequent analysis focused on the even parts alone.

We fitted these profiles to a precession model similar to the Kramer (1998) model to solve for details of the geometry and of the beam. However, the quality of our data enabled us to fit eleven different profile regions rather than just the profile peaks (see Figure 2). Figures 1 and 2 both demonstrate that the profile peaks have approached one another (as shown first by Kramer 1998) and the saddle has become more prominent, while the outer edges are virtually unchanged from 1981 to 1999. We found that we could not successfully fit a circular beam model to our data, nor one with a single value for ellipticity. Instead, we required a model where the north–south elongation *grows* with angular radius ρ from the beam symmetry axis. In our adopted model, the angular radius of equal-intensity contours is given by

$$\rho = \rho_0 \left[1 + \frac{(R - 1)\sigma^2}{\sigma_0^2 + \sigma^2} \right], \tag{1}$$

where σ is the impact parameter of the line of sight with respect to the beam axis, σ_0 is the characteristic impact parameter, ρ_0 is the characteristic angular radius, and R is the characteristic axial ratio. Note that $\rho \rightarrow \rho_0$ at low $|\sigma|$ and $\rho \rightarrow R\rho_0$

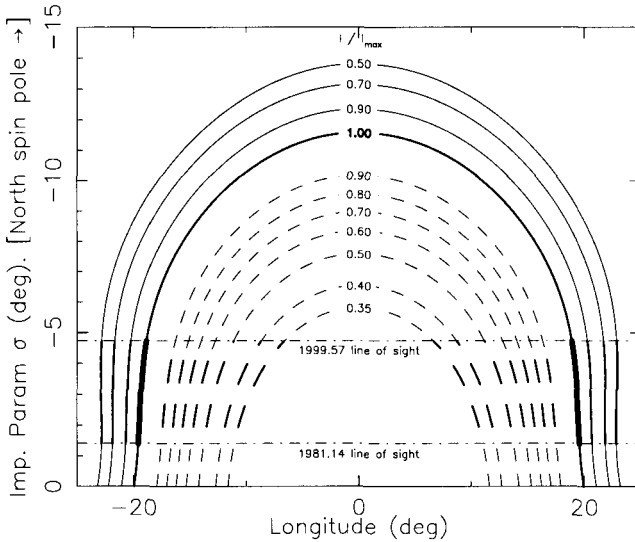


Figure 3. Two-dimensional elongated hollow-cone beam model.

at high $|\sigma|$. In our fitted model, $R = 1.62$, and $\sigma_0 = 7^\circ.18$. The equal-intensity curves of Figure 2 were calculated from this model, with σ allowed to vary while ρ_0 was held fixed. Simultaneously fitted precession parameters include the observable magnetic pole colatitude $\alpha = 156^\circ.3$, the orbital inclination $i = 156^\circ.3$, and the spin-orbit angular momentum misalignment angle $\delta = 22^\circ.1$.

4. Discussion

Figure 3 displays our fitted elongated beam model in two dimensions. The line of sight trajectories from the earliest (1981.14) and latest (1999.57) sessions are shown to emphasize that we have currently sampled only a limited range of impact parameters. Nevertheless it is apparent that we have sampled this pulsar's beam sufficiently to demonstrate that it is elongated in the latitude direction and that the elongation grows with radius from the beam axis.

References

- Istomin, Ya. N. 1991, *Soviet Ast. Lett.*, 17, 301
 Kramer, M. 1998, *ApJ*, 509, 856
 Taylor, J. H., & Weisberg, J. M. 1989, *ApJ*, 345, 434
 Weisberg, J. M., Romani, R. W., & Taylor, J. H. 1989, *ApJ*, 347, 1030
 Weisberg, J. M., & Taylor, J. H. 1992, in *IAU Colloq. 128, Magnetospheric Structure and Emission Mechanics of Radio Pulsars*, ed. T. H. Hankins, J. M. Rankin, & J. A. Gil (Zielona Gora: Pedagogical Univ. Press), 214